Received: 9 August 2019

DOI: 10.1002/mma.6890

RESEARCH ARTICLE

WILEY

Improved accuracy and convergence analysis of finite volume methods for particle fragmentation models

Jitraj Saha[1] | **Andreas Bück**[2]

[1]Department of Mathematics, National Institute of Technology Tiruchirappalli, Tiruchirappalli, Tamil Nadu, India

[2]Institute of Particle Technology (LFG), Friedrich-Alexander University Erlangen-Nürnberg, Erlangen, Germany

Correspondence
Jitraj Saha, Department of Mathematics, National Institute of Technology Tiruchirappalli, Tiruchirappalli 620 015, Tamil Nadu, India.
Email: jitraj@nitt.edu

Communicated by: M. Brokate

Funding information
National Institute of Technology Tiruchirappalli, Grant/Award Number: NITT/R&C/SEED GRANT/19-20/P-13/MATHS/JS/E1

In this work, two new number- and volume-consistent finite volume methods for the numerical solution of binary and multifragmentation problems are introduced. The new number-consistency is achieved by introducing a single weight function. Several benchmark problems of different complexity are solved to assess the accuracy. Mathematical convergence analysis suggests that both of the new methods are numerically second order convergent with respect to the grid size on uniform and nonuniform meshes.

KEYWORDS

conservative formulation, finite volume scheme, fragmentation equation, volume conservation, weight functions

MSC CLASSIFICATION

65R20

1 | INTRODUCTION

Fragmentation (or breakage) is the process of generating at least two new individual objects (fragments) from one initial object. If the object (particle) splits into exactly two fragments, the process is called binary fragmentation; otherwise, it is called multiple fragmentation. It occurs frequently in the processing of particulate solids. In comminution (grinding, milling), it is the required effect, in other applications, it is an unwanted side-effect, for example, the creation of dust particles due to attrition in pneumatic conveying of materials, which may lead to charge build-up and explosion hazard.[1,2] From a practical point of view, the extent and the property distribution are of key importance, for example, to assess the effectivity of a fragmentation process (e.g., comminution) or the magnitude of safety risks posed, for example, by dust handling.

In general, the population balance equation (PBE) is used to track the particle property distribution over time. Within the population balance framework,[3] fragmentation is modeled by integro-partial differential equations. Solutions of these equations then give information of the change of particle property distribution within the particular process. Several interesting mathematical studies on the behavior of the solutions during fragmentation events are available in the literature.[4,5] However, the PBE is often solved numerically as analytical results are available only for some particular simplified (benchmark) cases.

Finite volume schemes, for instance, the ones proposed in Bourgade and Filbet[6] (for binary fragments) and Kumar and Kumar[7] (for multiple fragments), are very often used to solve the integro-partial differential model equations. Since the schemes originate from a volume-conservative formulation, they are naturally consistent in terms of total volume of the particles in the system. However, a major drawback of these schemes is that they do not predict consistently the number of the particles, that is, too few or too many particles are present in the numerical solution than there are in reality.

Therefore, in industries like mining, minerals processing, or pharmaceutical industries,[8,9] numerical schemes are sought that not only are volume-consistent but also number-consistent.

In this work, two new finite volume schemes (MBF and MKK) are developed and tested that are both number- and volume-consistent. The basis of the development is the finite volume schemes proposed by Bourgade and Filbet[6] (BF) and Kumar and Kumar[7] (KK), which are volume-consistent only but have shown high efficiency in applications.

The manuscript is organized as follows: In the next section, the standard continuum models for fragmentation processes in the population balance framework are briefly presented. In Section 3, the two new finite volume schemes are developed from the methods of Bourgade and Filbet[6] and Kumar and Kumar.[7] Afterwards, numerical convergence analysis is performed. Section 5 illustrates the performance of the new methods by application to benchmark fragmentation problems. In Section 6, some conclusions are drawn, and an outlook on future work is presented.

2 | MATHEMATICAL MODELS OF FRAGMENTATION PROCESSES

The change of particle properties in fragmentation processes can be conveniently described on a macroscopic scale within the population balance framework:[3] Considering the particle volume x as particle property, a number distribution density $f(t,x)$ can be introduced in such a way that the number of fragments with volumes in the infinitesimal range $[x, x+\mathrm{d}x]$ is given by $f(t,x)\mathrm{d}x$. The property coordinate volume x is chosen as it allows to handle also nonspherical objects easily in the derivation of the balance equations. Furthermore, volume is additive, that is, $x = u + (x-u)$, a property that does not necessarily hold for other properties, for example, a particle diameter.

The resulting balance equations for $f(t,x)$ are very often partial differential or integro-partial differential equations which need to be solved numerically.

Before going into details, the continuous binary and the multiple fragmentation equations that can be used to describe fragmentation processes are introduced. Under the assumption of good mixing, and no spatial gradients, the binary fragmentation equation is written as[6]

$$\frac{\partial\left(xf(t,x)\right)}{\partial t} = \frac{\partial}{\partial x}\left[\int_0^x \int_{x-u}^{\infty} uF(u,v)f(t,u+v)\mathrm{d}v\mathrm{d}u\right], \tag{2.1}$$

along with the initial data

$$f_0(x) = f(0,x) \geq 0, \text{ for all } x \geq 0. \tag{2.2}$$

Here, $f(t,x)$ denotes the distribution of particle volume $x(\geq 0)$ at time $t(\geq 0)$, the fragmentation kernel $F(x,y)$ represents the rate at which a particle of volume $x+y$ splits into volumes x and y. In general, the kernel F is a nonnegative symmetric function of x and y. Its functional form depends on many parameters, for example, size/volume and a composition of the particle as well as operating parameters inducing the thermal or mechanical stress that leads to fragmentation. The natural purpose of the divergence formulation (2.1) is to give a precise account of the volume-conservation or mass-dissipation laws.

Following similar arguments, the divergence formulation of multiple fragmentation event is represented in Kumar and Kumar[7] as follows:

$$\frac{\partial\left(xf(t,x)\right)}{\partial t} = \frac{\partial}{\partial x}\left[\int_x^{\infty} \int_0^x uS(v)b(u,v)f(t,v)\mathrm{d}u\mathrm{d}v\right], \tag{2.3}$$

supported by the initial data (2.2). In the above equation, f is the number density function, $S(y)$ is the selection rate of particles of volume y to undergo fragmentation, and the breakage function $b(x,y)$ defines the distribution of smaller particles of volume x due to the breakup of larger particle of volume y. In general, $b(x,y)$ is considered to satisfy the following relations:

$$\int_0^y b(x,y)\mathrm{d}x = \nu(y), \text{ and } \int_0^y xb(x,y)\mathrm{d}x = y. \tag{2.4}$$

Here, $\nu(y)$ denotes the number of fragments in which a particle of volume y has split up. The second relation in the above equation is physically important, as it signifies that the total volume of all daughter particles x (fragments) equals the volume of the mother particle y. Again, the functions b, S and ν are specified by the material properties and the process conditions.

Total moments of the number density function are defined as

$$M_\alpha(t) = \int_0^\infty x^\alpha f(t,x)\mathrm{d}x, \tag{2.5}$$

where α denotes the order of the moment. Taking x as the particle volume, the zeroth moment represents the total number, and the first moment corresponds to the total volume of the particles in the system. Higher order moments, for example, $\alpha = 2, 3, \ldots$, do not bear much physical significance. Of some physical importance are the fractional moments stemming from $\alpha = 1/3$ and $\alpha = 2/3$: $M_{1/3}$ is proportional to the total length of all particles, and $M_{2/3}$ is proportional to the total surface area. Equivalence is achieved by scaling the values of $M_{1/3}$ and $M_{2/3}$ by a geometry-dependent shape factor.

Based on these observations, our objective is to formulate numerical methods which are number- and volume-consistent, that is, no particles and particle volumes are lost or created due to the numerical scheme while solving the mathematical model.

A particulate system obeys volume-conservation, if

$$\frac{dM_1(t)}{dt} = 0. \tag{2.6}$$

It can be verified that both the Equations (2.1) and (2.3) naturally satisfy the volume-conservation rule (2.6), when all the integrals exist finitely. Similarly, the temporal change of zeroth moment obtained from relation (2.1) is

$$\frac{dM_0(t)}{dt} = \frac{1}{2}\int_0^\infty f(t,x)\int_0^x F(x-y,y)\mathrm{d}y\mathrm{d}x, \tag{2.7}$$

and relation (2.3) gives

$$\frac{dM_0(t)}{dt} = \int_0^\infty S(x)f(t,x)\left[\nu(x)-1\right]\mathrm{d}x. \tag{2.8}$$

The derivation of relations (2.7) and (2.8) is given in Appendix A.

3 | DISCRETE FORMULATIONS

In order to apply a finite volume method, the volume scale of interacting particles is fixed. Consider the computational domain to be $\mathcal{D} :=]0, x_{\max}]$ and it is further discretized into $I(<\infty)$ subintervals $\Lambda_i :=]x_{i-1/2}, x_{i+1/2}]$, $i = 1, 2, \ldots, I$ such that $x_{1/2} = 0$ and $x_{I+1/2} = x_{\max}$. The midpoint of each Λ_i is denoted by x_i and is considered to be the cell representative (pivot). We assume that the meshes $(\Lambda_i)_i$ are either uniform or monotonically increasing, that is,

$$\Delta x_i \le \Delta x_{i+1}, \text{ for all } i = 1, 2, \ldots, I-1. \tag{3.1}$$

Further, let $\delta x := \min_i \Delta x_i$, $\Delta x := \max_i \Delta x_i$ such that there exists a positive constant γ satisfying

$$\frac{\Delta x}{\delta x} \le \gamma. \tag{3.2}$$

For the sake of convenience, we denote $g(t,x) := xf(t,x)$.

Let $\hat{g}_i(t)$ be the approximation of the cell average value of the particle mass density (or the solution g) on the cell Λ_i at time t. Mathematically it is defined as

$$\hat{g}_i(t) \approx \frac{1}{\Delta x_i}\int_{\Lambda_i} g(t,x)\mathrm{d}x. \tag{3.3}$$

Therefore, one can easily find the approximate particle number density as

$$\hat{f}_i(t) := \frac{\hat{g}_i(t)}{x_i}. \tag{3.4}$$

For notational simplicity, we drop the argument t. However, it should not be understood that $\hat{g}_i$ is independent of the time variable t. Since it is intended to predict both the zeroth and the first moment, their discrete formulations, which will be used in the later part of this study, are introduced. Therefore, analogous to the continuous formulations, the temporal change of the discrete zeroth moments corresponding to the binary fragmentation model (2.7) is written as

$$\frac{d}{dt}\sum_{i=1}^{I}\hat{f}_i\Delta x_i = \frac{1}{2}\sum_{i=1}^{I}\hat{f}_i\Delta x_i\sum_{k=1}^{i}\int_{x_{k-1/2}}^{p_k^i}F(x_i-x,x)\mathrm{d}x, \tag{3.5}$$

where

$$p_k^i := \begin{cases} x_k, & \text{when } k=i,\\ x_{k+1/2}, & \text{otherwise,}\end{cases} \tag{3.6}$$

and that of multiple fragmentation model (2.8) is given by

$$\frac{d}{dt}\sum_{i=1}^{I}\hat{f}_i\Delta x_i = \sum_{i=1}^{I}S_i\hat{f}_i\left[\nu(x_i)-1\right]\Delta x_i. \tag{3.7}$$

Here, $\nu(x_i)$ denotes the number of fragments produced during the fragmentation of particle having volume x_i. The temporal change of the first moment which also corresponds to the discrete volume-conservation law, is written for the binary and multiple fragmentation model as

$$\frac{d}{dt}\sum_{i=1}^{I}\hat{g}_i\Delta x_i = 0. \tag{3.8}$$

3.1 | MBF: Modified scheme of Bourgade and Filbet[6]

The semi-discrete form of the finite volume scheme approximating the fragmentation model (2.1) proposed by Bourgade and Filbet[6] is written as

$$\frac{d\hat{g}_i}{dt} = \frac{1}{\Delta x_i}\left[\mathcal{F}_{i+1/2}-\mathcal{F}_{i-1/2}\right], \tag{3.9}$$

where $\mathcal{F}$ is the numerical flux function at the ith cell boundaries and is defined as

$$\mathcal{F}_{i+1/2} := \sum_{j=1}^{i}\sum_{k=i+1}^{I}F_{j,k}\frac{x_j}{x_k}\hat{g}_k\Delta x_k, \tag{3.10}$$

with $F_{j,k} := \int_{x_{j-1/2}}^{p_j^k}F(x_k-x,x)\mathrm{d}x$, denoting the splitting of particles having volume k within the interval $]x_{j-1/2},p_j^k]$. For notational ease, we call the formulation (3.9) the *BF scheme*. The fluxes at the boundaries of domain D are taken as $\mathcal{F}_{1/2}=\mathcal{F}_{I+1/2}=0$.

Consider a sample problem and observe the efficiency of the BF scheme (3.9) for a constant fragmentation kernel with a monodisperse initial data.

From Figure 1, it is seen that the BF scheme (3.9) conserves the total volume of particles and also predicts the size distribution with good accuracy. This is evident from the fact that the BF scheme is originated directly from the continuous volume-conservative formulation (2.1). However, it fails to estimate the total particle number with good accuracy.

In order to overcome this situation, the following new model (MBF) based on the BF scheme is introduced:

$$\frac{d\hat{g}_i}{dt} = \frac{1}{\Delta x_i}\left[\tilde{\mathcal{F}}_{i+1/2}-\tilde{\mathcal{F}}_{i-1/2}\right], \tag{3.11}$$

where the flux at the cell boundaries is modified by introducing a weight function λ_k as follows:

$$\tilde{\mathcal{F}}_{i+1/2} := \sum_{j=1}^{i}\sum_{k=i+1}^{I}\lambda_k F_{j,k}\frac{x_j}{x_k}\hat{g}_k\Delta x_k, \tag{3.12}$$

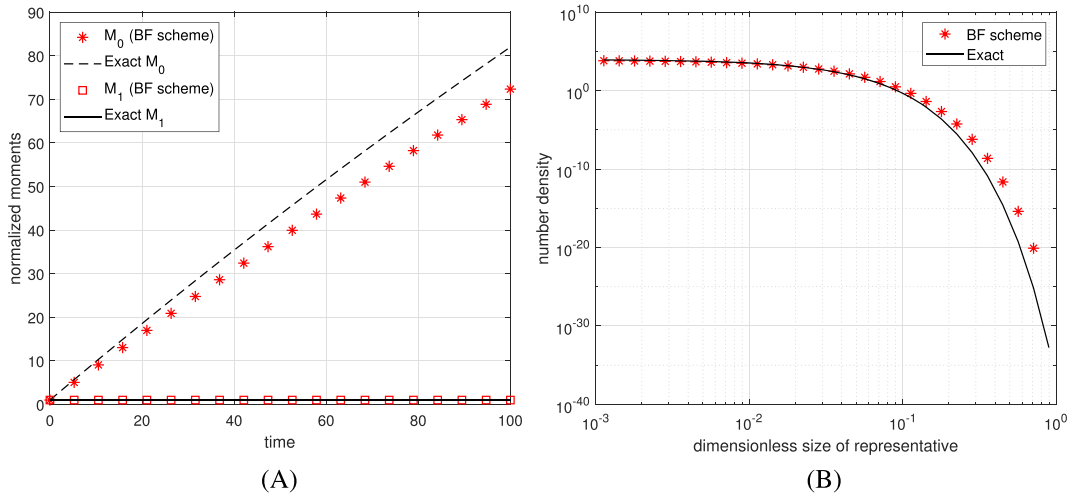

FIGURE 1 Computation of the BF scheme (2.5) for $F = 1$, $f_0 = \delta(x - 1)$ [Colour figure can be viewed at wileyonlinelibrary.com]

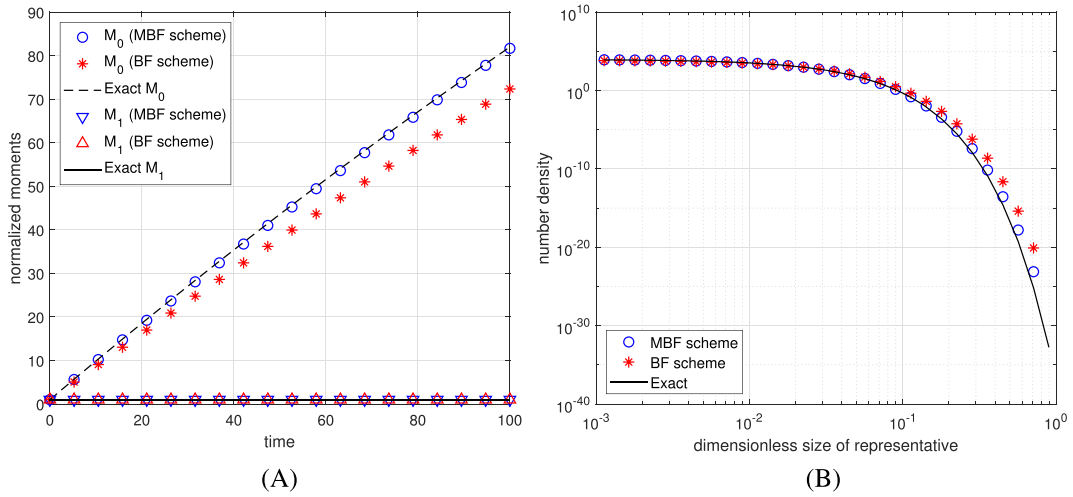

FIGURE 2 Comparison of the BF scheme (3.9) and MBF scheme (3.11) for $F = 1$, $f_0 = \delta(x - 1)$ [Colour figure can be viewed at wileyonlinelibrary.com]

and the weight is defined as

$$\lambda_k := \frac{\sum_{i=1}^{k} F_{i,k}}{2\sum_{i=1}^{k}\left(1 - \frac{x_i}{x_k}\right) F_{i,k}}, \tag{3.13}$$

with $\lambda_1 = 1$. Like in the BF scheme (3.9), the modified flux at the boundary points is considered to be zero, that is, $\tilde{F}_{1/2} = \tilde{F}_{I+1/2} = 0$.

Proposition 3.1. *The proposed method the MBF (3.11) obeys the discrete volume-conservation law (3.4) and also in line with the discrete zeroth moment relation (3.5).*

Proof. Multiplying both sides with Δx_i and taking sum over i on both sides of (3.11) yields

$$\frac{d}{dt}\sum_{i=1}^{I}(\hat{g}_i \Delta x_i) = 0.$$

Thus, the MBF scheme (3.11) obeys the discrete volume-conservation law.

Now, the discrete zeroth moment predicted by the MBF scheme (3.11) is calculated as follows: Multiplying both sides of (3.11) by $\frac{\Delta x_i}{x_i}$, then summing over i yields

$$\frac{d}{dt}\sum_{i=1}^{I}\hat{f}_i\Delta x_i = \sum_{i=1}^{I}\frac{1}{x_i}\left[\sum_{j=1}^{i}\sum_{k=i+1}^{I}\lambda_k F_{j,k}\frac{x_j}{x_k}\hat{g}_k\Delta x_k - \sum_{j=1}^{i-1}\sum_{k=i}^{I}\lambda_k F_{j,k}\frac{x_j}{x_k}\hat{g}_k\Delta x_k\right].$$

Simplifying and changing the order of summation in the first term and then interchanging indices, we get

$$\begin{aligned}
\frac{d}{dt}\sum_{i=1}^{I}\hat{f}_i\Delta x_i &= \sum_{k=1}^{I}\lambda_k\frac{\hat{g}_k\Delta x_k}{x_k}\sum_{i=1}^{k-1}\frac{1}{x_i}\sum_{j=1}^{i}x_j F_{j,k} - \sum_{k=1}^{I}\lambda_k\frac{\hat{g}_k\Delta x_k}{x_k}\sum_{i=1}^{k}\frac{1}{x_i}\sum_{j=1}^{i-1}x_j F_{j,k}\\
&= \sum_{k=1}^{I}\lambda_k\frac{\hat{g}_k\Delta x_k}{x_k}\sum_{i=1}^{k-1}\frac{1}{x_i}\left[\sum_{j=1}^{i}x_j F_{j,k} - \sum_{j=1}^{i-1}x_j F_{j,k}\right] - \sum_{k=1}^{I}\lambda_k\frac{\hat{g}_k\Delta x_k}{x_k}\sum_{j=1}^{k-1}\frac{x_j}{x_k}F_{j,k}\\
&= \sum_{k=1}^{I}\lambda_k\frac{\hat{g}_k\Delta x_k}{x_k}\sum_{i=1}^{k-1}F_{i,k} - \sum_{k=1}^{I}\lambda_k\frac{\hat{g}_k\Delta x_k}{x_k}\sum_{j=1}^{k-1}\frac{x_j}{x_k}F_{j,k}\\
&= \sum_{k=1}^{I}\lambda_k\frac{\hat{g}_k\Delta x_k}{x_k}\sum_{i=1}^{k}\left(1-\frac{x_i}{x_k}\right)F_{i,k}.
\end{aligned}$$

Recalling λ_i from (3.13) and substituting in the above relation, we get

$$\frac{d}{dt}\sum_{i=1}^{I}\hat{f}_i\Delta x_i = \frac{1}{2}\sum_{k=1}^{I}\hat{f}_k\Delta x_k\sum_{i=1}^{k}F_{i,k} = \frac{1}{2}\sum_{k=1}^{I}\hat{f}_k\Delta x_k\int_0^{x_k}F(x_k-x,x)\mathrm{d}x.$$

Thus, the discrete zeroth moment obtained from the MBF scheme (3.11) is in line with the relation (3.5). □

Thus it is verified that the new MBF scheme (3.11) predicts the total volume and the total number consistently. This is achieved by introducing a suitable weight function λ. An interesting feature of the weight function λ (3.13) is that it is always independent of time, whenever the fragmentation kernel is independent of time. Hence, all the required weights can be precomputed before solving the system of equations.

As a first test, the sample problem is considered and is solved by the BF scheme (3.9) and the MBF scheme (3.11). From the Figure 2, we observe that the weighted scheme (3.11) estimates the number density and the first moment as good as the BF scheme (3.9). In addition, the MBF scheme (3.11) predicts the evolution of total particle number with an improved accuracy as compared to the BF scheme (3.9).

In Section 5, more elaborate benchmark problems with complex fragmentation kernels are solved to evaluate the improvement in accuracy of the MBF scheme over the BF scheme.

To study the convergence, the newly proposed MBF scheme (3.11) is rewritten in the following form:

$$\frac{d\hat{\mathbf{g}}(t)}{dt} = \mathbf{B}\hat{\mathbf{g}}(t), \tag{3.14}$$

where $\hat{\mathbf{g}}(t) := \left[\hat{g}_1, \hat{g}_2, \ldots, \hat{g}_I\right]$ is the vector representation of the numerical solution of (3.11), and $\mathbf{B} = \left(b_{ij}\right)$ is an $I\times I$ matrix given by

$$\mathbf{B} := \begin{bmatrix}
\frac{d_{1,1-1/2}}{\Delta x_1} & \frac{d_{2,1-1/2}-d_{2,1+1/2}}{\Delta x_1} & \frac{d_{3,1-1/2}-d_{3,1+1/2}}{\Delta x_1} & \cdots & \frac{d_{I,1-1/2}-d_{I,1+1/2}}{\Delta x_1}\\
0 & \frac{d_{2,2-1/2}}{\Delta x_2} & \frac{d_{3,2-1/2}-d_{3,2+1/2}}{\Delta x_2} & \cdots & \frac{d_{I,2-1/2}-d_{I,2+1/2}}{\Delta x_2}\\
\vdots & \vdots & \vdots & \ddots & \vdots\\
0 & 0 & 0 & \cdots & \frac{d_{I,I-1/2}}{\Delta x_I}
\end{bmatrix}, \tag{3.15}$$

with

$$d_{k,i+1/2} := -\frac{\lambda_k}{x_k}\sum_{j=1}^{i}x_j F_{j,k}.$$

3.2 | MKK: Modified scheme of Kumar and Kumar[7]

In this section, the second, new number- and volume-consistent method is based on the following finite volume scheme proposed by Kumar and Kumar[7] approximating the multiple fragmentation problems,

$$\frac{d\hat{g}_i}{dt} = -\frac{1}{\Delta x_i}\left[\mathcal{J}_{i+1/2} - \mathcal{J}_{i-1/2}\right], \tag{3.16}$$

where

$$\mathcal{J}_{i+1/2} := -\sum_{k=i+1}^{I} \hat{g}_k \int_{\Lambda_k} \frac{S(\epsilon)}{\epsilon} \mathrm{d}\epsilon \int_0^{x_{i+1/2}} ub(u, x_k)\mathrm{d}u. \tag{3.17}$$

For further reference, the scheme (3.16) is called the *KK scheme*. Denote

$$\int_{\Lambda_k} \frac{S(\epsilon)}{\epsilon}\mathrm{d}\epsilon =: \mathcal{A}_k, \text{ and } \int_{\Lambda_j} ub(u, x_k)\mathrm{d}u =: \mathcal{B}_{jk}.$$

Similar to the previous case of binary fragmentation, the KK scheme (3.16) also obeys the volume conservation law:

$$\frac{d}{dt}\sum_{i=1}^{I} \hat{g}_i \Delta x_i = 0.$$

However, the KK scheme is not consistent in the discrete zeroth moment given by the relation (3.7). To show this, divide both sides of (3.16) by x_i and then take the sum over i to get

$$\begin{aligned}
\frac{d}{dt}\sum_{i=1}^{I} \hat{f}_i \Delta x_i &= \sum_{i=1}^{I} \frac{1}{x_i}\left[\sum_{k=i+1}^{I} \hat{g}_k \mathcal{A}_k \int_0^{x_{i+1/2}} ub(u, x_k)\mathrm{d}u \right.\\
&\quad \left. -\sum_{k=i}^{I} \hat{g}_k \mathcal{A}_k \int_0^{x_{i-1/2}} ub(u, x_k)\mathrm{d}u\right]\\
&= \sum_{k=1}^{I} \hat{g}_k \mathcal{A}_k \left[\sum_{i=1}^{k-1} \frac{1}{x_i}\int_0^{x_{i+1/2}} ub(u, x_k)\mathrm{d}u - \sum_{i=1}^{k} \frac{1}{x_i}\int_0^{x_{i-1/2}} ub(u, x_k)\mathrm{d}u\right]\\
&= \sum_{k=1}^{I} \frac{\hat{g}_k \mathcal{A}_k}{x_k} \left[\sum_{i=1}^{k-1} \frac{x_k}{x_i}\int_{x_{i-1/2}}^{x_{i+1/2}} ub(u, x_k)\mathrm{d}u - \int_0^{x_{k-1/2}} ub(u, x_k)\mathrm{d}u\right]\\
&= \sum_{k=1}^{I} \frac{\hat{g}_k \mathcal{A}_k}{x_k} \sum_{i=1}^{k} \left(\frac{x_k}{x_i} - 1\right) \mathcal{B}_{ik}.
\end{aligned}$$

Therefore, the KK scheme fails to produce a consistent estimate of the total particle number.

Therefore, a new finite volume method (MKK) on the basis of the KK scheme (3.16) is introduced to numerically solve multifragmentation models:

$$\frac{d\hat{g}_i}{dt} = -\frac{1}{\Delta x_i}\left[\tilde{\mathcal{J}}_{i+1/2} - \tilde{\mathcal{J}}_{i-1/2}\right]. \tag{3.18}$$

Here, the flux function $\tilde{\mathcal{J}}$ is defined as

$$\tilde{\mathcal{J}}_{i+1/2} := -\sum_{k=i+1}^{I} \omega_k \hat{g}_k \mathcal{A}_k \sum_{j=1}^{i} \mathcal{B}_{jk}, \tag{3.19}$$

where

$$\omega_k := \frac{S_k\left[\nu(x_k)-1\right]\Delta x_k}{\mathcal{A}_k\sum_{i=1}^{k}\left(\frac{x_k-x_i}{x_i}\right)\mathcal{B}_{ik}}, \tag{3.20}$$

with $\omega_1 = 1$.

Proposition 3.2. *The MKK scheme (3.18) obeys the volume conservation law (3.6) and is also consistent with the discrete zeroth moment (3.7).*

Proof. Calculating in a similar manner as done for the binary fragmentation and using the weight function ω_k (3.20) yields:

$$\frac{d}{dt}\sum_{i=1}^{I}\hat{g}_i\Delta x_i = 0, \text{ and } \frac{d}{dt}\sum_{i=1}^{I}\hat{f}_i\Delta x_i = \sum_{i=1}^{I}S_i\hat{f}_i\left[\nu(x_i)-1\right]\Delta x_i.$$

□

Thus, it is shown that the MKK scheme given by (3.18) estimates the discrete zeroth and first moments consistently. In the following section, we consider several sample problems to justify the improvement.

Contrary to the binary fragmentation case, the weight function ω_k (3.20) may depend on time. Only in the case of time-independent selection functions, the weights are constant and can be calculated before hand.

Similar to the MBF scheme (3.11), we rewrite the MKK scheme (3.18) as follows:

$$\frac{d\hat{\mathbf{g}}(t)}{dt} = \mathbf{C}\hat{\mathbf{g}}(t), \tag{3.21}$$

where $\hat{\mathbf{g}}(t) := \left[\hat{g}_1, \hat{g}_2, \ldots, \hat{g}_I\right]$ is the numerical solution of (3.18) in vector form, and $\mathbf{C} = \left(c_{ij}\right)$ is the $I \times I$ matrix defined by

$$\mathbf{C} := \begin{bmatrix} \frac{u_{1,1-1/2}}{\Delta x_1} & \frac{u_{2,1-1/2}-u_{2,1+1/2}}{\Delta x_1} & \frac{u_{3,1-1/2}-u_{3,1+1/2}}{\Delta x_1} & \cdots & \frac{u_{I,1-1/2}-u_{I,1+1/2}}{\Delta x_1} \\ 0 & \frac{u_{2,2-1/2}}{\Delta x_2} & \frac{u_{3,2-1/2}-u_{3,2+1/2}}{\Delta x_2} & \cdots & \frac{u_{I,2-1/2}-u_{I,2+1/2}}{\Delta x_2} \\ \vdots & \vdots & \vdots & \ddots & \vdots \\ 0 & 0 & 0 & \cdots & \frac{u_{I,I-1/2}}{\Delta x_I} \end{bmatrix}, \tag{3.22}$$

with

$$u_{k,i+1/2} := -\omega_k\mathcal{A}_k\sum_{j=1}^{i}\mathcal{B}_{j,k}.$$

4 | CONVERGENCE ANALYSIS

In the following study, we first recall some theorems and definitions from Kumar and Kumar[7] that will be used throughout this section. Since we have two semi-discrete formulations (i) the MBF scheme (3.14) and (ii) the MKK scheme (3.21), therefore, to avoid a confusion, we first present the definitions and theorems for the MBF scheme (3.14). However, all the definitions and theorems mentioned in Kumar and Kumar[7] are directly applicable for the MKK scheme (3.21).

Let $g_i(t)$ denotes the $i-$th cell average value of the exact solution of the Equation (2.1), that is

$$g_i(t) := \frac{1}{\Delta x_i}\int_{\Lambda_i} g(t,x)\mathrm{d}x, \text{ for } i = 1, 2, \ldots, I. \tag{4.1}$$

Let the discrete L^1 norm be defined by

$$\left\|\mathbf{g}(t)\right\| = \sum_{i=1}^{I}\left|g_i(t)\right|\Delta x_i. \tag{4.2}$$

Definition 4.1 (Spatial truncation error)**.** The spatial truncation error is defined by the residual left by substituting the exact solution vector $\mathbf{g}(t) := \left[g_1, g_2, \ldots, g_I\right]$ into Equation (3.14) as

$$\sigma(t) = \frac{d\mathbf{g}(t)}{dt} - \mathbf{B}\mathbf{g}(t). \tag{4.3}$$

The scheme is called to be consistent of order p if for $\Delta x \to 0$

$$\|\sigma(t)\| = \mathcal{O}\left(\Delta x^p\right), \text{ uniformly for all} 0 \le t \le T.$$

Definition 4.2 (Logarithmic norm)**.** The logarithmic norm of a matrix $\mathbf{A} \in \mathbb{R}^{m\times m}$ is defined as

$$\tilde{\mu}(\mathbf{A}) = \lim_{\tau\to 0} \frac{\|I + \tau\mathbf{A}\| - 1}{\tau}.$$

The logarithmic norm of a matrix $\mathbf{A}$ corresponding to $p = 1$ norms in $\mathbb{R}^m$ is given by

$$\tilde{\mu}(\mathbf{A}) = \max_j \left(a_{jj} + \sum_{i\neq j} |a_{ij}| \right).$$

Theorem 4.1. *If $\mathbf{A} \in \mathbb{R}^{m\times m}$ and $\beta \in \mathbb{R}$ then*

$$\tilde{\mu}(\mathbf{A}) \le \beta \iff \left\| e^{\mathbf{A}t} \right\| \le e^{\beta t}, \text{ for all } t \ge 0.$$

Definition 4.3. The semi-discrete system (3.14) is stable if

$$\left\| e^{\mathbf{B}t} \right\| \le K e^{\beta t} \text{ for} 0 \le t \le T,$$

holds for all grids with constant $K \ge 1$ and $\beta \in \mathbb{R}$ being independent of Δx.

Theorem 4.2 (Non-negativity)**.** *The solution of the linear semi-discrete system (3.14) is nonnegative if and only if*

$$b_{ij} \ge 0, \text{ for all } i \ne j,$$

where b_{ij} are the entries of the matrix $\boldsymbol{B}$.

4.1 | Convergence of MBF scheme

Theorem 4.3 (positivity, stability, and Consistency)**.** *Consider $F(x, y) \in C^2([0, x_{\max}] \times [0, x_{\max}])$ and $f(\cdot, x) \in C^2([0, x_{\max}])$. Then the semi-discrete MBF scheme (3.14) is second order accurate over uniform as well as monotonic nonuniform meshes satisfying (3.1).*

Proof. Positivity: Referring to the formulation (3.14), it can easily be seen that $d_{i,j-1/2} - d_{i,j+1/2} \ge 0$ for $1 \le i, j \le I$. Hence, using Theorem 4.2 positivity of the solution follows.

Consistency: In order to calculate the spatial truncation error, we recall the continuous formulation (2.1) and integrate it with respect to x over the cell Λ_i. Therefore, we get

$$\frac{dg_i}{dt} = \frac{1}{\Delta x_i}\left[\mathcal{G}\left(x_{i+1/2}\right) - \mathcal{G}\left(x_{i-1/2}\right)\right], \tag{4.4}$$

where $\mathcal{G}$ is the flux flow at the ith cell boundaries and is defined by

$$\mathcal{G}(x_{i+1/2}) := \int_0^{x_{i+1/2}} \int_{x_{i+1/2}-u}^{x_{\max}} uF(u,v)f(t,u+v)\mathrm{d}v\mathrm{d}u. \tag{4.5}$$

Rearranging the terms, we get

$$\mathcal{G}(x_{i+1/2}) = \int_0^{x_{i+1/2}} \int_{x_{i+1/2}}^{x_{\max}} uF(u,v-u)f(t,v)\mathrm{d}v\mathrm{d}u = \sum_{j=1}^{i}\int_{\Lambda_j}\sum_{k=i+1}^{I}\int_{\Lambda_k} uF(u,v-u)f(t,v)\mathrm{d}v\mathrm{d}u.$$

Using the midpoint quadrature formula, one can easily get

$$\mathcal{G}(x_{i+1/2}) = \mathcal{F}_{i+1/2} + \mathcal{O}\left(\Delta x^2\right), \tag{4.6}$$

where, $\mathcal{F}$ is the numerical flux defined in Equation (3.10). Next we recall the definition of the spatial truncation error (4.3), it reads as

$$\sigma_i(t) = \frac{1}{\Delta x_i}\left[\left(\mathcal{F}_{i+1/2} - \tilde{\mathcal{F}}_{i+1/2}\right) - \left(\mathcal{F}_{i-1/2} - \tilde{\mathcal{F}}_{i-1/2}\right)\right] + \mathcal{O}\left(\Delta x^2\right). \tag{4.7}$$

Considering the first two terms

$$\mathcal{F}_{i+1/2} - \tilde{\mathcal{F}}_{i+1/2} = \sum_{j=1}^{i}\sum_{k=i+1}^{I}\left[1-\lambda_k\right]\frac{x_j}{x_k}F_{j,k}\hat{g}_k\Delta x_k,$$

we proceed to estimate the term $(1-\lambda_k)$. We have

$$\begin{aligned}(1-\lambda_k) &= \frac{2\sum_{l=1}^{k}\int_{x_{l-1/2}}^{p_l^k}(x_k-x_l)\,F\left(x_k-x,x\right)\mathrm{d}x - x_k\int_0^{x_k}F(x_k-x,x)\mathrm{d}x}{2\sum_{l=1}^{k}\int_{x_{l-1/2}}^{p_l^k}(x_k-x_l)\,F\left(x_k-x,x\right)\mathrm{d}x}\\ &= \frac{x_k\int_0^{x_k}F(x_k-x,x)\mathrm{d}x - 2\sum_{l=1}^{k}x_l\int_{x_{l-1/2}}^{p_l^k}F\left(x_k-x,x\right)\mathrm{d}x}{2\sum_{l=1}^{k}\int_{x_{l-1/2}}^{p_l^k}(x_k-x_l)\,F\left(x_k-x,x\right)\mathrm{d}x}.\end{aligned}$$

It can easily be calculated that the fragmentation kernel F satisfies (for details, please refer to Saha et al[10]) the following condition:

$$x_k\int_0^{x_k}F(x_k-x,x)\mathrm{d}x = 2\int_0^{x_k}xF(x_k-x,x)\mathrm{d}x.$$

Using the above relation, we get

$$(1-\lambda_k) = \frac{\sum_{l=1}^{k}\int_{x_{l-1/2}}^{p_l^k}(x-x_l)\,F\left(x_k-x,x\right)\mathrm{d}x}{\sum_{l=1}^{k}\int_{x_{l-1/2}}^{p_l^k}(2x-x_l)\,F\left(x_k-x,x\right)\mathrm{d}x}.$$

Using the midpoint and the right-endpoint quadrature formulas together with the fact that $F(0,x) = F(x,0) = 0$, we get the numerator as

$$\int_{x_{l-1/2}}^{p_l^k} (x - x_l)\, F(x_k - x, x)\mathrm{d}x = \mathcal{O}\left(\Delta x_l^3\right),$$

and the denominator as

$$\int_{x_{l-1/2}}^{p_l^k} (2x - x_l)\, F(x_k - x, x)\mathrm{d}x = \frac{x_k}{2}\int_0^{x_k} F(x_k - x, x)\mathrm{d}x + \mathcal{O}\left(\Delta x_l^3\right).$$

Since $F \in C^2([0, x_{\max}] \times [0, x_{\max}])$, so $\int_0^{x_k} F(x_k - x, x)\mathrm{d}x$ is bounded. Moreover, we can find that

$$\frac{\sum_{l=1}^{k} \Delta x_l}{x_k} = \frac{x_{k+1/2}}{x_k} = \frac{x_k + \Delta x_k/2}{x_k} = 1 + \frac{\Delta x_k}{2x_k}$$

lies between 1 and 2. Therefore, summing up all the above mentioned arguments along with the condition (3.2), one can easily obtain that

$$(1 - \lambda_k)\, F_{j,k} = \mathcal{O}\left(\Delta x_k^3\right),$$

which implies

$$\mathcal{F}_{i+1/2} - \tilde{\mathcal{F}}_{i+1/2} = \mathcal{O}\left(\Delta x^2\right),$$

and hence,

$$\|\sigma(t)\| = \sum_{i=1}^{I} |\sigma_i(t)|\, \Delta x_i = \mathcal{O}\left(\Delta x^2\right). \tag{4.8}$$

Stability: We compute the logarithmic norm of the matrix **B**. Since all the nondiagonal elements of the matrix **B** are nonnegative, the logarithmic norm takes the form

$$\tilde{\mu}(\mathbf{B}) := \max_j \left(\sum_i b_{ij}\right).$$

Substituting $d_{k,1-1/2} = 0$ for all k, we get

$$\sum_i b_{ij} = \sum_{i=2}^{j} d_{j,j-1/2}\left(\frac{1}{\Delta x_i} - \frac{1}{\Delta x_{i-1}}\right).$$

Since the mesh considered is nondecreasing in nature, therefore, it follows that $\sum_i b_{ij} \leq 0$, and hence $\tilde{\mu}(\mathbf{B}) \leq 0$. Consequently,

$$\left\| e^{\mathbf{B}t} \right\| \leq 1,$$

which ensures the stability of the scheme, with the stability constant $\beta = 0$. □

4.2 | Convergence of the MKK scheme

Theorem 4.4 (positivity, stability, and consistency)**.** *Consider* $f(\cdot, x), S(x) \in C^2([0, x_{\max}])$ *and* $b \in C^2(]0, x_{\max}] \times [0, x_{\max}])$. *Then the semi-discrete MKK scheme (3.14) is second order accurate over the uniform as well as the nonuniform meshes satisfying (3.1).*

Proof. *Positivity:* It can easily be obtained that $u_{i,j-1/2} - u_{i,j+1/2} \geq 0$ for $1 \leq i, j \leq I$. Hence, the Theorem 4.2 implies the positivity of the solution.

Consistency: We first integrate the continuous formulation (2.3) with respect to x over the cell Λ_i and get

$$\frac{dg_i}{dt} = -\frac{1}{\Delta x_i}\left[\mathcal{M}\left(x_{i+1/2}\right) - \mathcal{M}\left(x_{i-1/2}\right)\right], \tag{4.9}$$

where

$$\mathcal{M}(x_{i+1/2}) := \int_{x_{i+1/2}}^{x_{\max}} \int_{0}^{x_{i+1/2}} uS(v)b(u,v)f(t,v)\mathrm{d}u\mathrm{d}v. \tag{4.10}$$

Now referring to Kumar and Kumar,[7] one can infer that

$$\mathcal{M}(x_{i+1/2}) = \mathcal{J}_{i+1/2} + \mathcal{O}\left(\Delta x^2\right). \tag{4.11}$$

Therefore, the definition of spatial truncation error reads as

$$\sigma_i(t) = -\frac{1}{\Delta x_i}\left[\left(\mathcal{J}_{i+1/2} - \tilde{\mathcal{J}}_{i+1/2}\right) - \left(\mathcal{J}_{i-1/2} - \tilde{\mathcal{J}}_{i-1/2}\right)\right] + \mathcal{O}\left(\Delta x^2\right).$$

Considering the first two terms

$$\tilde{\mathcal{J}}_{i+1/2} - \mathcal{J}_{i+1/2} = \sum_{k=i+1}^{I} (\omega_k - 1)\,\hat{g}_k \mathcal{A}_k \sum_{j=1}^{i} \mathcal{B}_{j,k}, s$$

we estimate the term $(\omega_k - 1)$ using the midpoint and right-endpoint quadrature formulas.

$$\begin{aligned}
(\omega_k - 1) &= \frac{S_k\left[\nu(x_k) - 1\right]\Delta x_k}{\mathcal{A}_k \sum_{i=1}^{k}\left(\frac{x_k - x_i}{x_i}\right)\mathcal{B}_{ik}} - 1 \\
&= \frac{\left[\nu(x_k) - 1\right] - \sum_{i=1}^{k}\left(\frac{x_k - x_i}{x_i}\right)\mathcal{B}_{ik}}{\sum_{i=1}^{k}\left(\frac{x_k - x_i}{x_i}\right)\mathcal{B}_{ik}} + \mathcal{O}\left(\Delta x_k^3\right) \\
&= \frac{x_k \int_0^{x_k} b(u,x_k)\mathrm{d}u - \sum_{i=1}^{k} x_i \int_{x_{i-1/2}}^{p_i^k} b(u,x_k)\mathrm{d}u - \sum_{i=1}^{k}(x_k - x_i)\int_{x_{i-1/2}}^{p_i^k} b\,(u,x_k)\,\mathrm{d}u}{\sum_{i=1}^{k}(x_k - x_i)\int_{x_{i-1/2}}^{p_i^k} b\,(u,x_k)\,\mathrm{d}u} \\
&\quad + \mathcal{O}\left(\Delta x_k^3\right) \\
&= \frac{\sum_{i=1}^{k}(x_k - x_i)\,b\,(u,x_k)\,\mathrm{d}u - \sum_{i=1}^{k}(x_k - x_i)\,b\,(u,x_k)\,\mathrm{d}u}{\sum_{i=1}^{k}(x_k - x_i)\,b\,(u,x_k)\,\mathrm{d}u} + \mathcal{O}\left(\Delta x_k^3\right).
\end{aligned}$$

Therefore, we get

$$(\omega_k - 1)\sum_{j=1}^{i}\mathcal{B}_{j,k} = \mathcal{O}\left(\Delta x_k^3\right).$$

Hence,

$$\mathcal{J}_{i+1/2} - \tilde{\mathcal{J}}_{i+1/2} = \mathcal{O}\left(\Delta x^2\right), \tag{4.12}$$

and consequently,

$$\|\sigma(t)\| = \sum_{i=1}^{I} \sigma_i(t)\Delta x_i = \mathcal{O}\left(\Delta x^2\right). \tag{4.13}$$

Stability: We now proceed in a similar manner as done for the MBF scheme and compute the logarithmic norm of the matrix $\mathbf{C}$. Since all the nondiagonal elements of the matrix $\mathbf{C}$ are nonnegative, the logarithmic norm takes the form

$$\tilde{\mu}(\mathbf{C}) := \max_j \left(\sum_i c_{ij} \right).$$

Substituting $u_{k,1-1/2} = 0$ for all k and considering the nondecreasing nature of the mesh, we get

$$\sum_i c_{ij} = \sum_{i=2}^{j} u_{j,j-1/2} \left(\frac{1}{\Delta x_i} - \frac{1}{\Delta x_{i-1}} \right) \leq 0.$$

Hence $\tilde{\mu}(\mathbf{C}) \leq 0$. Consequently,

$$\left\| e^{\mathbf{C}t} \right\| \leq 1,$$

ensures the stability of the scheme, with the stability constant $\beta = 0$. □

5 | NUMERICAL RESULTS

In this section, several benchmark problems are considered to compare accuracy and performance of the two new methods the MBF (3.11) and the MKK (3.18) with their basis, the BF (3.9) and the KK (3.16) schemes, respectively. Furthermore, the numerical order of convergence is calculated for both schemes. In all test problems, the following conditions apply:

1. The computational domain considered is $\mathcal{D} := [10^{-9}, 1]$ and is further discretized into 30 nonuniform subintervals using the geometric recurrence relation $x_{i+1/2} = r x_{i-1/2}$, where $r > 1$.
2. All the problems are written in semi-discrete form and the adaptive time step solver ode45 (MATLAB) is used to solve them numerically.
3. Final time $T = 100$ (dimensionless).
4. Dimensionless values of all the concerned quantities are considered during the computations.
5. All the benchmark cases are supported with the monodispersed initial data, that is,

$$f_0(x) = \delta(x - x_I) = \begin{cases} 1, \text{ when } x = x_I, \\ 0, \text{ otherwise.} \end{cases}$$

5.1 | Binary fragmentation: Benchmark cases

5.1.1 | Benchmark case 1

Consider the volume-dependent fragmentation kernel $F(x, y) = x + y$. The exact solution of this problem is available in Ziff and McGrady.[11] Figure 3 clearly depicts the improved accuracy of the MBF scheme (3.11) over the BF scheme (3.9).

In Table 1, the *numerical order of convergence* (NOC) of the MBF scheme on uniform and nonuniform meshes is presented. For the details on computing the relative errors and the NOC, the readers are referred to Kumar and Kumar.[7] In both cases, it is observed that the MBF scheme shows the second order convergence.

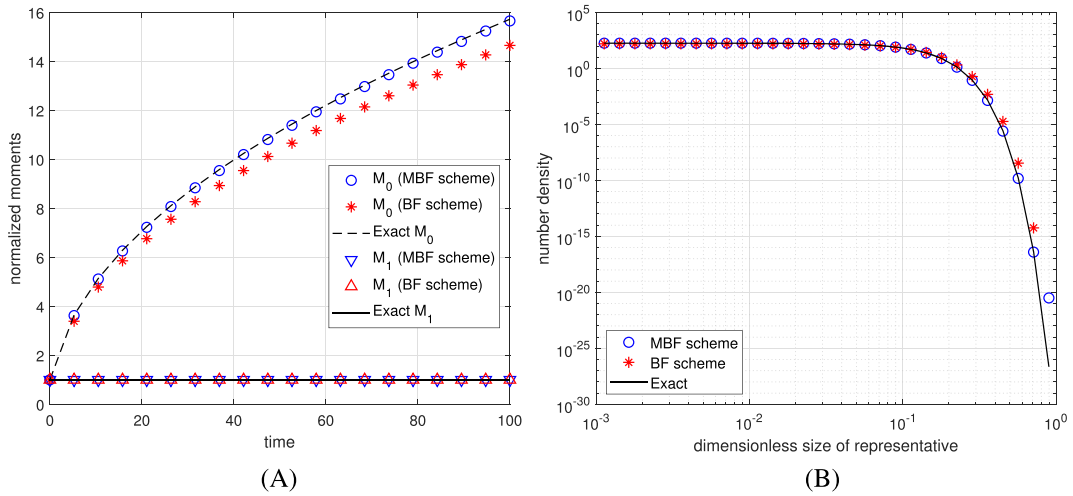

(A) (B)

FIGURE 3 Numerical results for benchmark case 1 with kernel $F = x + y$ [Colour figure can be viewed at wileyonlinelibrary.com]

TABLE 1 NOC of the MBF scheme for benchmark case 1 with kernel $F = x + y$

(a) Uniform Mesh			(b) Nonuniform Mesh		
Grid Points	**Relative Error**	**NOC**	**Grid Points**	**Relative Error**	**NOC**
30	0.0020	-	30	0.0789	-
60	0.0005	1.9311	60	0.0204	1.7782
120	0.0001	1.9614	120	0.0052	1.8823
240	0.0000	1.9693	240	0.0013	1.9450
480	0.0000	1.9472	480	0.0003	1.9654

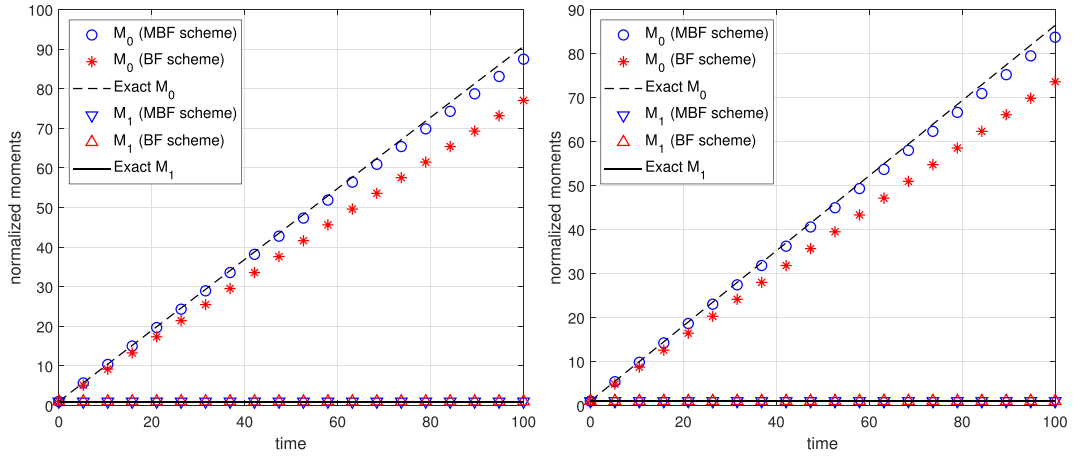

(A) Kernel F_1 (B) Kernel F_2

FIGURE 4 Numerical moments for benchmark case 2 with kernels F_1 and F_2 [Colour figure can be viewed at wileyonlinelibrary.com]

5.1.2 | Benchmark case 2

Consider the two complex volume-dependent fragmentation kernels, (i) $F_1(x, y) = 6\frac{xy}{(x+y)^2}$ and (ii) $F_2(x, y) = 30\frac{x^2y^2}{(x+y)^4}$. The exact solutions of the problems for these kernels are not available in the literature, but the zeroth and the first moments can be computed in their closed form. In Figure 4, the numerical moments are presented against their exact values. Figure 4A corresponds to the kernel F_1 and Figur 4B corresponds to the kernel F_2. As before, an improved accuracy of the MBF scheme over the BF scheme is observed in both cases.

Table 2 reports the numerical order of convergence of the MBF scheme for the problem with kernel F_1, and Table 3 reports the same for kernel F_2. For both the problems, the MBF scheme exhibits the second order convergence.

5.2 | Multiple fragmentation: Benchmark cases

5.2.1 | Benchmark case 3

Consider the multifragment problem with $S(x) = x^2$ and $b(x, y) = \frac{2}{y}$. The exact solution of this problem is available in Ziff.[12]

TABLE 2 NOC of the MBF scheme for benchmark case 2 with kernel F_1

(a) Uniform Mesh			(b) Nonuniform Mesh		
Grid Points	**Relative Error**	**NOC**	**Grid Points**	**Relative Error**	**NOC**
30	-	-	30	-	-
60	0.2071	-	60	0.2101	-
120	0.0647	1.6774	120	0.0735	1.5153
240	0.0185	1.8042	240	0.0187	1.9730
480	0.0048	1.9447	480	0.0047	2.0026

TABLE 3 NOC of the MBF scheme for benchmark case 2 with kernel F_2

(a) Uniform Mesh			(b) Nonuniform Mesh		
Grid Points	**Relative Error L_1**	**NOC**	**Grid Points**	**Relative Error L_1**	**NOC**
30	-	-	30	-	-
60	1.2720	-	60	1.2694	-
120	0.2678	2.2476	120	0.2737	2.2136
240	0.0635	2.0769	240	0.0632	2.1156
480	0.0153	2.0510	480	0.0151	2.0614

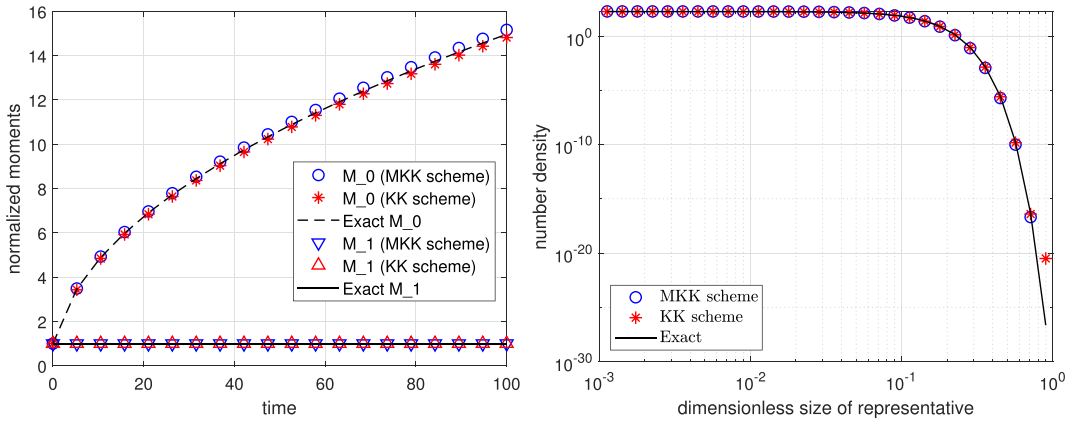

FIGURE 5 Numerical results for benchmark case 3 with $S = x^2$, $b = 2/y$ [Colour figure can be viewed at wileyonlinelibrary.com]

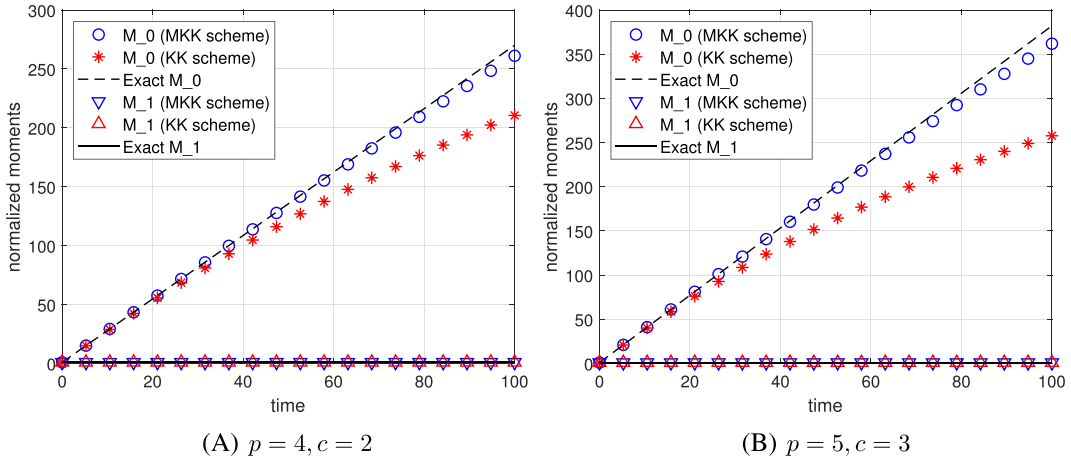

FIGURE 6 Numerical moments for benchmark case 4 [Colour figure can be viewed at wileyonlinelibrary.com]

TABLE 4 NOC of the MKK scheme for benchmark case 3 with $S = x^2$, $b = 2/y$

(a) Uniform Mesh			(b) Nonuniform Mesh		
Grid Points	**Relative Error**	**NOC**	**Grid Points**	**Relative Error**	**NOC**
30	0.0779	-	30	0.0779	-
60	0.0213	1.6726	60	0.0203	1.7707
120	0.0055	1.8707	120	0.0051	1.8777
240	0.0014	1.9472	240	0.0013	1.9433
480	0.0003	1.9752	480	0.0003	1.9682

TABLE 5 NOC of the MKK scheme for benchmark case 4 with $p = 4$ and $c = 2$

(a) Uniform Mesh			(b) Nonuniform Mesh		
Grid Points	**Relative Error**	**NOC**	**Grid Points**	**Relative Error**	**NOC**
30	-	-	30	-	-
60	1.0649	-	60	1.0780	-
120	0.2254	2.2402	120	0.2196	2.2953
240	0.0563	2.0006	240	0.0524	2.0668
480	0.0141	1.9991	480	0.0128	2.0287

TABLE 6 NOC of the MKK scheme for benchmark case 4 with $p = 5$ and $c = 3$

(a) Uniform Mesh			Nonuniform Mesh		
Grid Points	**Relative Error**	**NOC**	**Grid Points**	**Relative Error**	**NOC**
30	-	-	30	-	-
60	0.7071	-	60	0.7358	-
120	0.1633	2.1141	120	0.1485	2.3089
240	0.0405	2.0120	240	0.0355	2.0633
480	0.0101	2.0000	480	0.0087	2.0294

Figure 5 shows the results obtained by application of the KK scheme (3.16) and the MKK scheme (3.18). In comparison to the KK scheme an improved estimate of the total particle number is calculated by the MKK scheme.

Table 4 reports the relative error and the numerical order of convergence of the MKK scheme (3.18) for uniform and nonuniform meshes. The MKK scheme shows the second order convergence.

5.2.2 | Benchmark problem 4

Consider the linear selection function $S(x) = x$ and the general breakage function

$$b(x, y) = \frac{px^c(y-x)^{c+(c+1)(p-2)}[c+(c+1)(p-1)]!}{y^{c+(c+1)(p-1)}[c!][c+(c+1)(p-2)]!}$$

mentioned in Kumar and Kumar.[7] Here, p and c are the parameters indicating the number of fragments produced during breakage and the shape factor of the particles, respectively. An analytical result for the distribution function f is not available; however, zeroth and first-order moments can be evaluated analytically (with the first-order moment given directly from the initial data). In the following example, two sets of parameter values are considered: $p = 4, c = 2$ and $p = 5, c = 3$.

Figure 6 presents the exact and the numerical moments obtained from the KK scheme and the MKK scheme. Figure 6A corresponds to the problem with parameters $p = 4$ and $c = 2$, and Figure 6B corresponds to $p = 5$ and $c = 3$. In both cases, the improved accuracy of the MKK scheme over the KK scheme is clearly observed.

The numerical order of convergence of the MKK scheme over uniform and nonuniform meshes is tabulated in Tables 5 and 6 for the two parameter sets. In all cases, the MKK scheme is numerically second order convergent.

6 | CONCLUSIONS AND OUTLOOK

In this article, two new finite volume schemes for binary and multi-fragmentation models were introduced. Both methods are number- and volume-consistent, as opposed to the original methods proposed by Bourgade and Filbet[6] (for binary fragmentation) and Kumar and Kumar[7] (for multiple fragmentation) which are only volume-consistent.

Newly proposed methods, the MBF (3.11) and the MKK (3.18), retain the computational properties of their basis methods with respect to efficiency and robustness. Additionally, both methods are numerically second-order convergent, that

is, very good estimates can be obtained using only a small number of pivots. This renders the new methods attractive for dynamic optimization and control of fragmentation processes as these heavily rely on fast forward simulation of the underlying mathematical models. In future work, the approach will be extended to multi-dimensional fragmentation problems.

ACKNOWLEDGEMENTS

We are thankful to the anonymous referee for providing valuable suggestions which have resulted in the considerable improvement of the manuscript. The author JS thank the NITT project grant (NITT/R&C/SEED GRANT/19−20/P−13/MATHS/JS/E1) for their funding support during this work.

CONFLICTS OF INTEREST

This work does not have any conflicts of interest.

ORCID

Jitraj Saha https://orcid.org/0000-0002-8864-5537
Andreas Bück https://orcid.org/0000-0002-7803-1486

REFERENCES

1. Kalman H. Attrition control by pneumatic conveying. *Powder Technol*. 1999;104(3):214–220.
2. Kalman H. Attrition of powders and granules at various bends during pneumatic conveying. *Powder Technol*. 2000;112(3):244–250.
3. Ramkrishna D. *Population Balances: Theory and Applications to Particulate Systems in Engineering*: Academic Press; 2000.
4. McGuinness GC, Lamb Wilson, McBride AC. On a class of continuous fragmentation equations with singular initial conditions. *Math Methods Appl Sci*. 2011;34(10):1181–1192.
5. Banasiak J, Joel LO, Shindin S. Analysis and simulations of the discrete fragmentation equation with decay. *Math Methods Appl Sci*. 2018;41(16):6530–6545.
6. Bourgade JP, Filbet F. Convergence of a finite volume scheme for coagulation-fragmentation equations. *Math Comput*. 2008;77(262):851–882.
7. Kumar R, Kumar J. Numerical simulation and convergence analysis of a finite volume scheme for solving general breakage population balance equations. *Appl Math Comput*. 2013;219(10):5140–5151.
8. Ishii T, Matsushita M. Fragmentation of long thin glass rods. *J Phys Soc Japan*. 1992;61(10):3474–3477.
9. Fuerstenau DW, De A, Kapur PC. Linear and nonlinear particle breakage processes in comminution systems. *Int J Mineral Process*. 2004;74:S317–S327.
10. Saha J, Kumar J, Heinrich S. A volume-consistent discrete formulation of particle breakage equation. *Comput Chem Eng*. 2017;97:147–160.
11. Ziff RM, McGrady ED. The kinetics of cluster fragmentation and depolymerisation. *J Phys A*. 1985;18(15):3027–3037.
12. Ziff RM. New solutions to the fragmentation equation. *J Phys A*. 1991;24(12):2821–2828.

How to cite this article: Saha J, Bück A. Improved accuracy and convergence analysis of finite volume methods for particle fragmentation models. *Math Meth Appl Sci*. 2020;1–18. https://doi.org/10.1002/mma.6890

APPENDIX A: TEMPORAL EVOLUTION OF ZEROTH MOMENT

The volume-conservative formulation of binary fragmentation equation is written as

$$\frac{x\partial f(t,x)}{\partial t} = \frac{\partial}{\partial x}\left[\int_0^x \int_{x-u}^{\infty} uF(u,v)f(t,u+v)\mathrm{d}v\mathrm{d}u\right]. \tag{A.1}$$

Using Leibnitz' rule of integration under differentiation, Equation (A.1) reduces to

$$\frac{\partial f(t,x)}{\partial t} = \int_0^{\infty} F(x,y)f(t,x+y)\mathrm{d}y - \frac{1}{2}\int_0^x F(x-y,y)f(t,x)\mathrm{d}y. \tag{A.2}$$

Now, integrating (A.2) with respect to x and then performing some mathematical computations, we get

$$\frac{dM_0(t)}{dt} = \frac{1}{2}\int_0^\infty f(t,x)\int_0^x F(x-y,y)\mathrm{d}y\mathrm{d}x.$$

On the other hand, the volume-conservative formulation of the multiple fragmentation is written as

$$\frac{x\partial f(t,x)}{\partial t} = \frac{\partial}{\partial x}\left[\int_x^\infty \int_0^x uS(v)b(u,v)f(t,v)\mathrm{d}u\mathrm{d}v\right]. \tag{A.3}$$

In a similar manner, using Leibnitz rule of integration under differentiation, Equation (A.3) reduces to

$$\frac{df(t,x)}{dt} = \int_x^\infty S(y)b(x,y)f(t,y)\mathrm{d}y - S(x)f(t,x). \tag{A.4}$$

Therefore, from (A.4), it can easily be obtained that

$$\frac{dM_0(t)}{dt} = \int_0^\infty S(x)f(t,x)\left[\nu(x)-1\right]\mathrm{d}x.$$